JACS
JOURNAL OF THE AMERICAN CHEMICAL SOCIETY
Article
pubs.acs.org/JACS

Activation of Cell-Penetrating Peptides with Ionpair−π Interactions and Fluorophiles

Nicolas Chuard,[†] Kaori Fujisawa,[†,§] Paola Morelli,[†] Jacques Saarbach,[†] Nicolas Winssinger,[†] Pierangelo Metrangolo,[‡] Giuseppe Resnati,[‡] Naomi Sakai,[†] and Stefan Matile*[,†]

[†]Department of Organic Chemistry, University of Geneva, CH-1211 Geneva, Switzerland

[‡]NFMLab, Department of Chemistry, Materials and Chemical Engineering "Giulio Natta", Politecnico di Milano, via Mancinelli 7, I-20131 Milan, Italy

Supporting Information

ABSTRACT: In this report, we elaborate on two new concepts to activate arginine-rich cell-penetrating peptides (CPPs). Early on, we have argued that repulsion-driven ion-pairing interactions with anionic lipids account for their ability to move across hydrophobic cell membranes and that hydrophobic anions such as pyrenebutyrate can accelerate this process to kinetically outcompete endosomal capture. The original explanation that the high activity of pyrenebutyrate might originate from ionpair−π interactions between CPP and activator implied that replacement of the π-basic pyrene with polarized push−pull aromatics should afford more powerful CPP activators. To elaborate on this hypothesis, we prepared a small collection of anionic amphiphiles that could recognize cations by ionpair−π interactions. Consistent with theoretical predictions, we find that parallel but not antiparallel ionpair−π interactions afford operational CPP activators in model membranes and cells. The alternative suggestion that the high activity of pyrenebutyrate might originate from self-assembly in membranes was explored with perfluorinated fatty acids. Their fluorophilicity was expected to promote self-assembly in membranes, while their high acidity should prevent charge neutralization in response to self-assembly, i.e., generate repulsion-driven ion-pairing interactions. Consistent with these expectations, we find that perfluorinated fatty acids are powerful CPP activators in HeLa cells but not in model membranes. These findings support parallel ionpair−π interactions and repulsion-driven ion pairing with self-assembled fluorophiles as innovative concepts to activate CPPs. These results also add much corroborative support for counterion-mediated uptake as the productive mode of action of arginine-rich CPPs.

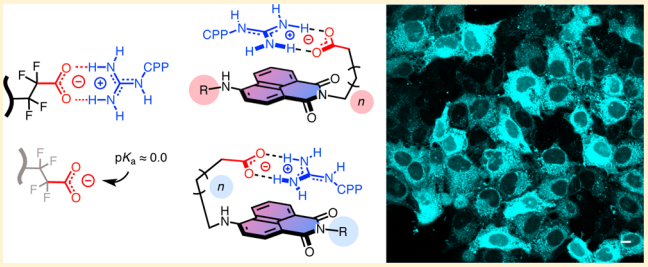

INTRODUCTION

Since their discovery in the late 1980s, the question how arginine-rich cell-penetrating peptides (CPPs) and their mimics move across cell membranes has caused intense debates in chemistry and biology.[1,2] After all, oligomers such as the fluorescently labeled octaarginine **1** used in this study are hydrophilic polycations (Figure 1A). They could not be expected to pass a hydrophobic membrane barrier as if it would not be there. Intrigued by a puzzling cation selectivity observed with arginine-rich synthetic pores,[3] we proposed early on that repulsion-driven ion-pairing interactions account for the productive mode of action of CPPs.[4] These most important interactions originate from the poor acidity of the guanidinium cation.[2] When brought into close proximity, the more acidic ammonium cations can eliminate charge repulsion by release of protons, i.e., reduction of the pK_a of all proximal ammonium cations except for one (Figure 1B). This proximity effect is operational throughout biology (e.g., class I aldolases).[2] With the less acidic guanidinium cations, proton release is essentially excluded in neutral water. The only remaining solution to minimize intramolecular charge repulsion in guanidinium-rich oligomers are counterions (Figure 1C). As a result of this proximity effect, counterions are bound tightly, but their exchange remains fast. In other words, repulsion-driven ion-pairing interactions ensure that CPPs will never be alone, but the nature of their counterions can change easily. For cellular uptake, CPPs will thus arrive at lipid bilayer membranes together with hydrophilic counterions such as phosphates or chlorides. Counterion exchange with anionic lipids will bind the CPPs to the cell membrane (Figure 1D). CPPs with sufficient activity will cross the membrane through micellar pores (Figure 1E).[2,5] These transient pores are dynamic enough to let large substrates pass and to heal once the CPPs have passed through. In the cytosol, CPPs detach from the membrane by counterion exchange with intracellular polyanions (Figure 1F). If ion-pairing mediated translocation is slow (k_t, Figure 1D), then kinetically competing endocytosis (k_e) dominates. Also in such cases, i.e., $k_e > k_t$, repulsion-driven ion-pairing translocation contributes to endosomal escape. This mode of action applies to arginine-rich CPPs and their models, particularly oligoarginines. Their activity is dependent on size, cargo, concentration,

Received: June 17, 2016
Published: August 29, 2016

DOI: 10.1021/jacs.6b06253
J. Am. Chem. Soc. 2016, 138, 11264−11271

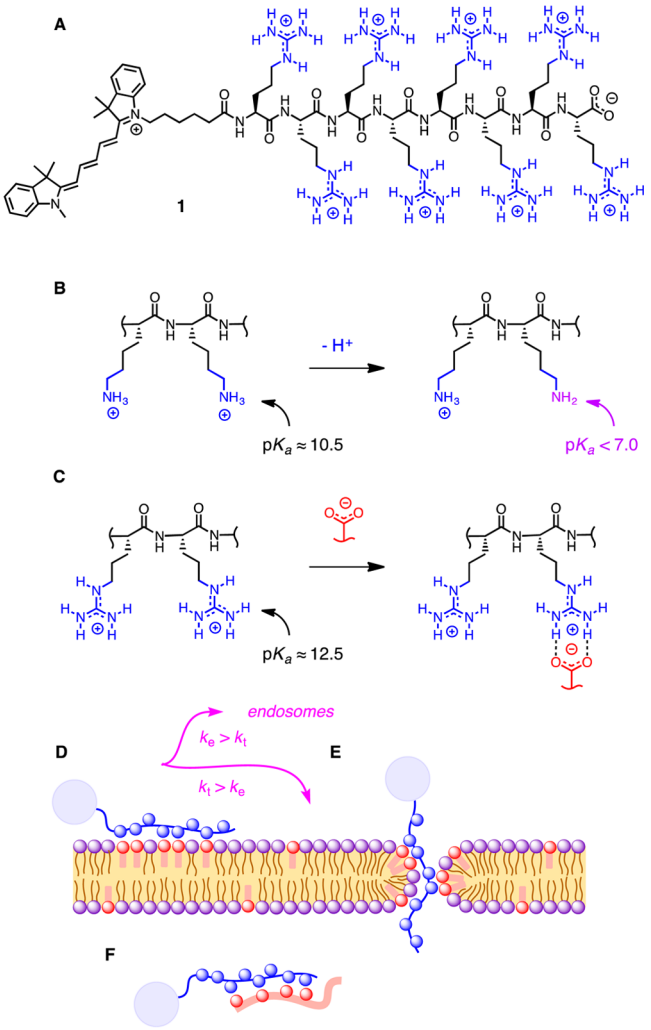

Figure 1. (A) Structure of the fluorescently labeled Cy5-CPP **1** used in this study. (B, C) Repulsion-driven ion-pairing interactions: The more acidic ammonium cations minimize charge repulsion between proximal lysine residues by deprotonation (B), and the less acidic guanidinium cations have to minimize charge repulsion between proximal arginine residues with repulsion-driven ion-pairing interactions (C). (D–F) The productive mode of action of CPPs: Counterion exchange with anionic lipids (or CPP activators, red) to bind to the outer membrane surface (D), formation of and translocation through transient dynamic micellar pores (E), and release by counterion exchange with internal hydrophilic polyions (F); kinetic competition from endocytosis (k_e) occurs if repulsion-driven ion-pairing translocation is slow (k_t).

and cell type.[1,2] Their cytotoxicity usually increases with concentration and number of guanidinium cations per oligo-/polymer.[1,2,6] Cell-penetrating poly(disulfide)s (CPDs) have been introduced recently to address this important problem with CPPs.[2,6]

The concept of counterion-mediated function with repulsion-driven ion-pairing interactions[2,4] has been not only introduced to explain the productive mode of action of arginine-rich CPPs but also applied to explain the voltage gating of potassium channels[7] and to create conceptually new sensors[2,8] and other responsive organic materials.[9]

For cellular uptake, the concept of repulsion-driven ion-pairing interactions implied that counterions other than the intrinsic anionic lipids could be used to activate CPPs.[2,4] Reminiscent of catalysts, CPP activators have been conceived to accelerate direct translocation across lipid bilayer membranes and thus kinetically outcompete endocytosis. Toward this end, many hydrophobic anions have been characterized as CPP activators in bulk (U tube, identifying counterion-activated CPPs as anion carriers[4]) and model membranes (dye-loaded vesicles).[2,4,10−12] Activities have been found to depend on the nature of both the CPPs and the CPP activators. Particularly attractive are the perfectly planar carboxylate-guanidinium pairs,[2,4] naturally including assistance from preorganized hydrogen bonding.[10]

Until recently, pyrenebutyrate **2** was the only counterion known to activate CPPs in a broad variety of cells (Figure 2).[13]

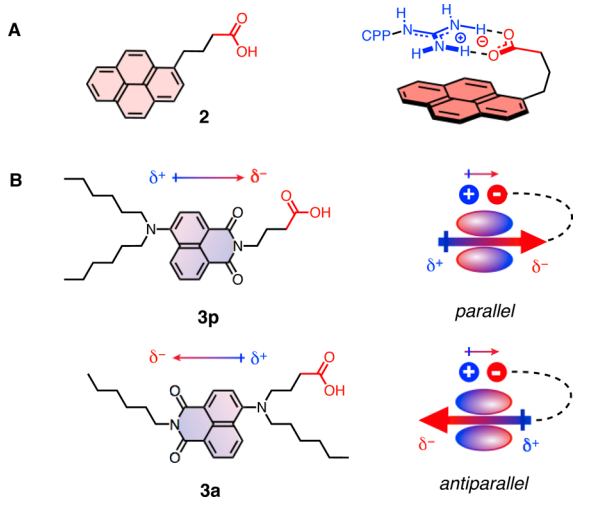

Figure 2. (A) The originally proposed structure of CPPs bound to pyrenebutyrate **2**. (B) Activators **3** could operate with parallel (**p**) and antiparallel (**a**) ionpair–π interactions on push–pull surfaces. They are defined by the direction of the push–pull dipoles (blue-to-red arrows, with partial charges) relative to orientation of the ion pair on their π surface (red and blue circles, small arrows).

The mode of activation has originally been explained with repulsion-driven ion-pairing on the electron-rich pyrene surface (Figure 2A).[4] The directionality of the resulting complex could possibly orient the CPPs more toward the interior of the membrane and thus facilitate the formation of transient micellar pores (Figure 1E). The originally proposed structure of the complex between CPP and activator **2** has recently been recognized as one of the rare examples of operational ionpair–π interactions in biology (Figure 2A).[14] However, the introduction of ionpair–π interactions also suggested that pyrenebutyrate activators should be far from perfect. Electron-rich π surfaces such as the one of pyrene are π basic, characterized by a negative quadrupole moment Q_{zz} in the z direction perpendicular to the plane and inward in-plane dipoles from donating substituents. This situation is suited to attract cations to the π surface.[15] For anion–π interactions, π-acidic surfaces with $Q_{zz} > 0$ and outward in-plane dipoles from withdrawing substituents are required.[16] To accommodate both an anion and a cation on the same aromatic surface, polarized push–pull surfaces with both π-acidic and π-basic side should be ideal (Figure 2B).[14]

In ionpair–π interactions, the orientation of the ion pair can be parallel or antiparallel with regard to the dipole of the push–pull system (Figure 2B). Recent insights from covalent systems indicated that parallel ionpair–π interactions are stronger than antiparallel ionpair–π interactions.[12,14] These findings sug-

DOI: 10.1021/jacs.6b06253
J. Am. Chem. Soc. 2016, 138, 11264–11271

gested that push−pull aminonaphthalimides (ANIs) **3p** designed for parallel ionpair−π interactions should be better CPP activators than antiparallel activators **3a** and should also be better than pyrenebutyrate **2**. Very recent preliminary results in model vesicles were consistent with these admittedly high expectations.[12]

CPP activators other than pyrenebutyrate **2** that work in cells have been reported very recently.[11] Namely, several ordinary fatty acids, essentially inactive at physiological conditions, have been shown to activate CPPs under more basic conditions. This finding suggested that fatty acid activators are not sufficiently deprotonated under neutral conditions, which in turn implies that they self-assemble in the membrane (see below).

Stimulated by these recent findings, we decided to more systematically explore the possibility to activate CPPs with parallel ionpair−π interactions on push−pull surfaces on the one hand and self-assembled activators on the other. In the following, we report the design, synthesis, and evaluation of a small collection of new activators. Experimental support is provided that parallel but not antiparallel ionpair−π interactions on push−pull surfaces might contribute to CPP activation, and perfluorinated fatty acids are introduced as remarkably powerful supramolecular CPP activators.

RESULTS AND DISCUSSION

Design. The design of ionpair−π activators **4**−**16** was based on pyrenebutyrate **2** and parallel and antiparallel ionpair−π activators **3a** and **3p** (Figure 3).[12] The shortcomings of

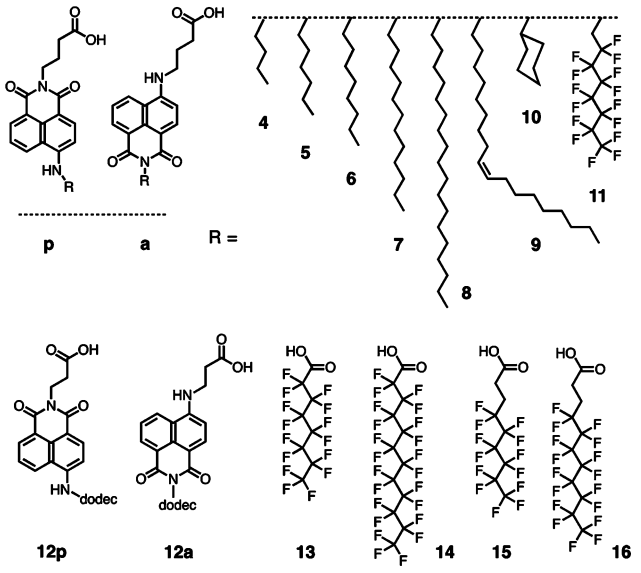

Figure 3. Structure of amphiphiles tested as CPP activators.

ionpair−π activators **3** are (i) poor push−pull polarization, because of a weak, twisted tertiary amine donor and (ii) inconsistent attachment of alkyl chains, making the amphiphilicity of the two constitutional isomers incomparable. To overcome these deficiencies, the collection of ionpair−π activators **4**−**11** was designed based on the central motif **a** and **p** arranged for antiparallel and parallel ionpair−π interactions, respectively. Activators **12** were of interest as controls with spacers between carboxylate on the π surface that are too short to fold into correct Leonard turns.[17] Fluorophiles[18] **13**−**16** were added to the collection to elaborate on activator self-assembly in lipid bilayer membranes.

Synthesis. The Cy5-labeled octaarginine **1** was synthesized by automated solid-phase synthesis (Figure 1A, Schemes S1 and S2). Activators **2** and **13**−**16** were commercially available, and all other activators were easily accessible in a few steps following the procedures developed previously for the original ionpair−π activators **3** (Figure 3, Schemes 1 and S3−S10). The

Scheme 1. Synthesis of Ionpair−π Activators 7a and 7p[a]

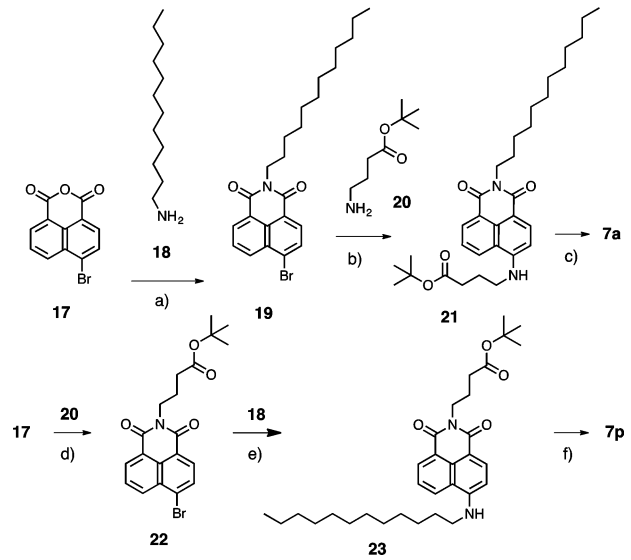

[a](a) EtOH, 90 °C, 15 h, 34%; (b) DMSO, TEA, 90 °C, 3 d, 72%; (c) TFA, CH_2Cl_2, rt, 2 h, 50%; (d) TEA, DMF, 2 h, μW, 52%; (e) 90 °C, 15 h, 79%; (f) TFA, CH_2Cl_2, rt, 2 h, 79%.

synthesis of one of the most interesting pair of activators, i.e., **7**, is outlined in Scheme 1. All details on synthesis and compound characterization can be found in the Supporting Information.[19]

CPP Activation in Vesicles. Activities in the model membranes were determined with the CF assay.[4] For these experiments, large unilamellar vesicles (LUVs) composed of egg yolk phosphatidylcholine (EYPC) were loaded with carboxyfluorescein (CF). Intravesicular CF concentrations were selected high enough to ensure self-quenching. CF export then results in fluorescence recovery due to local dilution.

In a typical experiment, CF emission was followed during the addition of first the activator, then polyarginine (pR) as simplest possible CPP mimic, and finally a detergent to destroy the vesicles for calibration (Figure 4A). Significant increases in emission before CPP addition identify activators that act as detergents. This can be observed for most activators[4] at sufficiently high concentrations; studies on CPP activation naturally have to focus on sublytic concentrations. Fluorescence kinetics for CPP activation were repeated with different concentrations, and the results were analyzed in dose response curves (Figure 4B). The activator characteristics obtained from Hill analysis are the maximal activity Y_{max} and the EC_{50}, which is the activator concentration needed to observe 50% of Y_{max} (Table 1, Figure 5).

The Y_{max} obtained for different activators varied broadly. The Y_{max} = 97% of the parallel ionpair−π activator **7p**, for example, revealed excellent activity (Figures 5A, 4B, red, ○, Table 1, entry 5). On the other hand, the Y_{max} = 14% observed for antiparallel ionpair−π activator **7a** (Figures 5A, 4B, blue ●, Table 1, entry 15) and Y_{max} = 21% for perfluorinated fatty acid **14** (Figures 5A, 4B, green △, Table 1, entry 22) indicated that

DOI: 10.1021/jacs.6b06253
J. Am. Chem. Soc. 2016, 138, 11264−11271

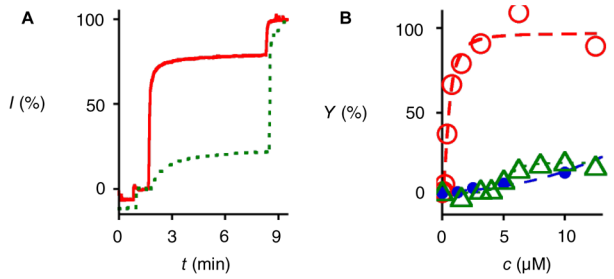

Figure 4. (A) Changes in CF emission I (λ_{ex} 492 nm, λ_{em} 517 nm) in CF-loaded EYPC LUVs (62.5 μM EYPC) as a function of time during the addition of activators **7p** (red, solid) or **14** (green, dashed) at t = 50 s (12.5 μM), pR (250 nM) at t = 100 s (I = 0%) and excess triton X-100 at t = 500 s for final calibration (I = 100%). (B) Dependence of final activity Y of pR (right before lysis in A) on the concentration of activators **7p** (red ○), **7a** (blue ●), and **14** (green △, with curve fit to Hill equation).

Table 1. Characteristic Parameters for CPP Activators in Vesicles Determined by Hill Analyses[a]

	activators[b]	Y_{max} (%)[c]	EC_{50} (μM)[d]	n[e]
1	**3p**[f]	61 ± 4	1.05 ± 0.05	2.1 ± 0.2
2	**4p**	9	inactive	
3	**5p**	87 ± 3	6.2 ± 0.2	3.8 ± 0.6
4	**6p**	66 ± 2	1.18 ± 0.07	2.4 ± 0.3
5	**7p**	97 ± 5	0.54 ± 0.09	1.8 ± 0.5
6	**8p**	24 ± 3	6 ± 1	1.3 ± 0.2
7	**9p**	27 ± 1	2.6 ± 0.2	1.9 ± 0.2
8	**10p**	59 ± 3	30 ± 1	4.4 ± 0.7
9	**11p**	70 ± 10	0.31 ± 0.08	1.8 ± 0.7
10	**12p**	68 ± 4	1.2 ± 0.2	4 ± 1
11	**3a**[f]	75[g]	3.6 ± 0.2	1.8 ± 0.2
12	**4a**	3	inactive	
13	**5a**	58[g]	19 ± 1	3.0 ± 0.6
14	**6a**	36[g]	15 ± 3	1.9 ± 0.7
15	**7a**	14	inactive	
16	**8a**	19 ± 1	3.5 ± 0.1	2.8 ± 0.2
17	**9a**	33 ± 9	30 ± 8	4 ± 3
18	**10a**	12	inactive	
19	**11a**	25	inactive	
20	**12a**	32[g]	28 ± 1	2.3 ± 0.2
21	**13**	21 ± 1	61 ± 8	5 ± 4
22	**14**	21 ± 1	5.1 ± 0.3	8 ± 2
23	**15**	7	inactive	
24	**16**	14	inactive	

[a]Determined using eq S2.[19] Hill analyses were not applied to those with low Y_{max} values. Errors are of curve fit. [b]Activators, see Figures 2 and 3. [c]Maximal activity. [d]Effective concentration to reach 50% activity of Y_{max}. [e]Hill coefficient. [f]From ref 12. [g]Maximum observed Y before the onset of the detergent effect. Hill analyses were made assuming Y_{max} = 100%.

these CPP activators are essentially inactive in vesicles. The apparent EC_{50} = 5.1 ± 0.3 μM obtained for **14** was obviously nearly meaningless considering this inacceptable Y_{max} = 21% (Figures 5B, 4B, green △, Table 1, entry 22), whereas the excellent Y_{max} = 97% identified the EC_{50} = 0.54 ± 0.09 μM measured for **7p** as a meaningful value (Figures 5B, 4B, red ○, Table 1, entry 5).

All new CPP activators were characterized in vesicles following this procedure (Table 1). The found activities Y_{max} were ordered as a function of the calculated log P, that is the

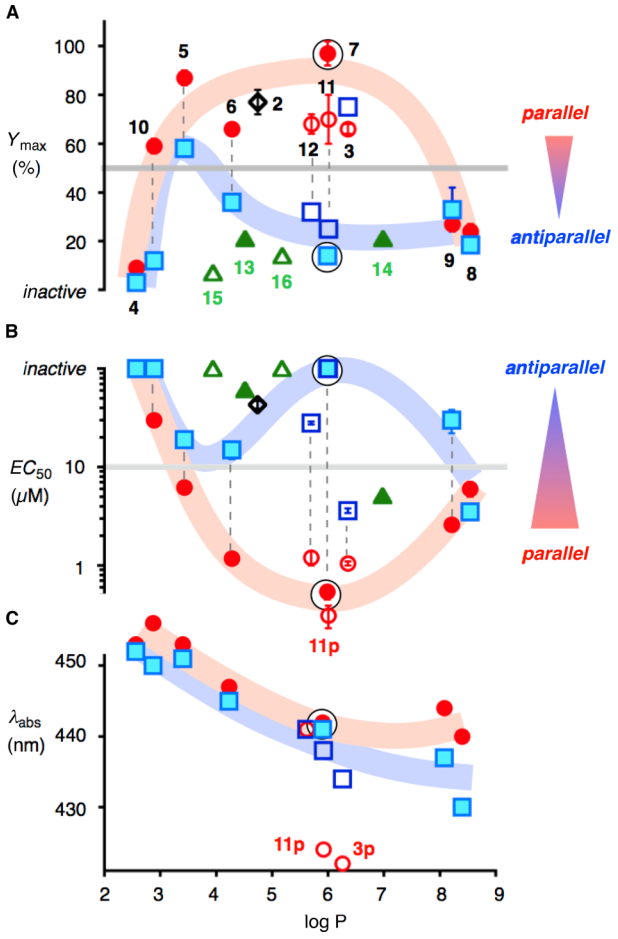

Figure 5. (A) Maximal activity Y_{max} and (B) effective concentration EC_{50} in vesicles as a function of the calculated log P, i.e., the hydrophobicity of the CPP activators estimated from their structure. From Hill analyses of dose response curves (Figure 4B). (C) Maxima in absorption spectra of ANI activators in EYPC LUVs. ANI activators **a** series: red circles; **p** series: blue squares; fluorinated fatty acids: green triangles; pyrenebutyrate: black diamonds; irregular or control compounds: open symbols. Isomers **a** and **p** are connected by gray dashed lines. Trend lines are added for activators **4**–**10**.

hydrophobicity of the activator (Figure 5A). Y_{max} ≥ 50% was defined as range of meaningful activity (Figure 5A, gray line). In addition, EC_{50} = 10 μM was considered as an appropriate limit of meaningful activities (Figure 5B, gray line). Activators **4**–**11** feature a flexible Leonard turn[17] to position the carboxylate on the aromatic surface (Figure 6). In the series **p**, the carboxylate is above the imide acceptor to support CPP binding by parallel ionpair–π interactions. In constitutional

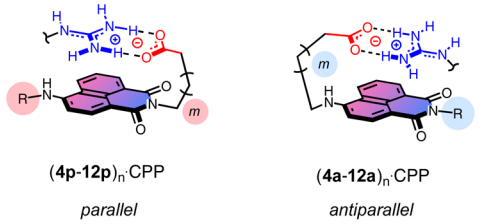

Figure 6. CPP activators **4**–**11** (m = 1) and **12** (m = 0) that can possibly operate with parallel (left) and antiparallel (right) ionpair–π interactions.

DOI: 10.1021/jacs.6b06253
J. Am. Chem. Soc. 2016, 138, 11264–11271

isomers **a**, the carboxylate is above the amine donor for antiparallel ionpair–π interactions with CPPs. In the series **4**–**8**, these parallel and antiparallel isomers were equipped with linear alkyl tails of increasing length from C4 to C18 (Figure 3). This collection was complemented with unsaturated oleyl tails in **9** because of their importance in the delivery of siRNA[2] and a cycloalkyl tail in **10**.

In CF-loaded vesicles, all parallel ionpair–π activators showed excellent Y_{max} except for the hydrophilic and hydrophobic extremes, i.e., **4p**, **8p** and **9p** (Figure 5A, red circles, Table 1, entries 1–10). In sharp contrast, most antiparallel ionpair–π activators were essentially inactive, except for the original **3a** and **5a** (Figure 5A, blue squares, Table 1, entries 11–20).

The trends found with Y_{max} were overall nicely reproduced with the EC_{50}. Except for extreme log *P*, parallel ionpair–π activators **p** were all very active (EC_{50} < 10 μM, Figure 5B, red circles), whereas their antiparallel constitutional isomers **a** showed much less convincing activities (Figure 5B, blue squares).

The original pyrenebutyrate **2** was special in the sense that high Y_{max} = 77% coincided with an EC_{50} = 43 ± 4 μM (Figures 5A and B, black diamonds). This unusually poor effective concentration was consistent with weak ionpair–π interactions on the π-basic pyrene surface (Figure 2).

Controls **12** with a shortened turn were characterized by less distinct behavior. The EC_{50} = 1.2 ± 0.2 μM of the most relevant **12p** was slightly less than expected from the hydrophobicity (Figure 5B). This slight underperformance was consistent with less than perfect turns to place the carboxylates on the push–pull surface (Figure 6). Previous results with shortened turns in anion–π catalysis confirmed that it would be unreasonable to expect larger changes from the removal of one carbon in the turn.[17]

Interestingly, the original **3a** with weakened push–pull system and disturbed amphiphilicity was the best among the otherwise consistently inactive antiparallel ionpair–π activators **a** (Figure 5A, B). In all controls with less than perfect architecture, i.e., **3** and **12**, the difference between EC_{50}'s for parallel and antiparallel ionpair–π interactions was less pronounced compared to the general trends (Figure 5A, B, red and blue lines).

Hill coefficients should be interpreted carefully because they increase not only with the stoichiometry but also with the instability of the formed complexes.[20] With all activators, Hill coefficients *n* were much smaller than expected for stoichiometric ion pairing (Table 1). These observations support that CPP–activator complexes are as stable as expected and that stoichiometric ion pairing with all the 33–99 guanidinium groups in pR is presumably not necessary to mediate its passage across the bilayer membrane. Within meaningful $Y_{max} \geq 50\%$, highest *n* were found for too hydrophilic activators (**5p**, **6p**, **10p**) and too short spacers (**12p**, Table 1, Figure 5A). These observations were consistent with less stable ionpair–π complexes formed in more polar environments and with incorrect turns.

With correct Leonard turns[17] and meaningfully balanced intermediate hydrophobicity, the difference in activity between parallel and antiparallel ionpair–π activators was overall much larger and more consistent than expected (Figure 5A, B, red vs blue lines). Nearly identical absorption maxima found for the constitutional isomers in vesicles suggested that their localization in membranes is similar (Figure 5C). Namely, with increasing hydrophobicity of the ionpair–π activators, the absorption maxima of both isomers shifted steadily to the blue, from almost 460 nm down to almost 430 nm. Considering the positive solvatochromism of the push–pull chromophore,[12] this trend indicated that with increasing overall hydrophobicity of the activators, the ANI core penetrates deeper in the hydrophobic core of the membrane. Similar location of parallel and antiparallel ionpair–π activators in the membrane (Figure 5C) suggested that the observed dramatic differences in CPP activation (Figure 5A, B) do not originate from differences in partitioning. This conclusion was in excellent agreement with operational parallel and dysfunctional antiparallel ionpair–π interactions in CPP activators that are otherwise almost identical (Figure 6).

The only significant exception from the general blue shift of ionpair–π activators with increasing hydrophobicity concerned **3p** and **11p** (Figure 5C). Their absorption in vesicles appeared about 20 nm more hypsochromic than expected from their hydrophobicity. These blue shifts probably originate from the twisted push–pull system in **3p** and self-assembly of fluorous **11p**, rather than particularly deep partitioning into the membrane.

Interestingly, polyfluorinated activators **13**–**16** were essentially inactive in vesicles, independent of the length of their tails and the basicity of their carboxylates (Figure 5A, B, green triangles). Hybrids **11** behaved more like ionpair–π rather than fluorous activators, i.e., parallel **11p** was active, while antiparallel **11a** was not. Polyfluorinated activator **11p** was slightly more active than expected from the general trend (Figure 5B, red lines), its EC_{50} = 310 ± 80 nM was the best of the entire collection (Table 1, entry 9).

CPP Activation in Cells. The uptake of fluorescently labeled octaarginine **1** into HeLa Kyoto cells in the absence and the presence of ionpair–π activators and fluorophiles was examined using confocal laser scanning microscopy (CLSM). The cells were incubated first with the activators for 5 min and then with 1 μM Cy5-CPP **1** for another 15 min at 37 °C in the standard Leibovitz medium (commercially available for cell culture in CO_2-free atmosphere). Then the cells were washed with PBS containing heparin (20 U/mL)[21] and Leibovitz medium to remove reversibly bound CPPs. Activators were mostly used at 10 μM, cell death could usually be observed above 20 μM, increasing with increasing concentration, dependent on the nature of the activator.

In the absence of activators, HeLa cells incubated with Cy5-CPP **1** showed the punctate fluorescence characteristic for endosomal capture (Figure 7A). Moreover, fluorescence intensities were overall relatively weak. Nearly identical images were obtained with antiparallel ionpair–π activator **7a** (Figure 7B). In clear contrast, some of the cells preincubated with activator **7p** showed exceptionally bright fluorescence after incubation with Cy5-CPP **1**, staining all over within the cells (Figure 7C). Interestingly, two extreme populations of cells could be observed, together with examples in-between. A significant minority of highly fluorescent cells (Figure 7C) alternated with a majority of others that showed weak emission from endosomes only, as for uptake of Cy5-CPP **1** in the absence of activators **7p** (Figure 7A). The overall appearance of the cells was similar to the original findings with pyrenebutyrate.[13]

The observed trends were consistent with results in CF-loaded vesicles (Figure 5). They supported that parallel ionpair–π activators interact better with the positively charged

DOI: 10.1021/jacs.6b06253
J. Am. Chem. Soc. 2016, 138, 11264–11271

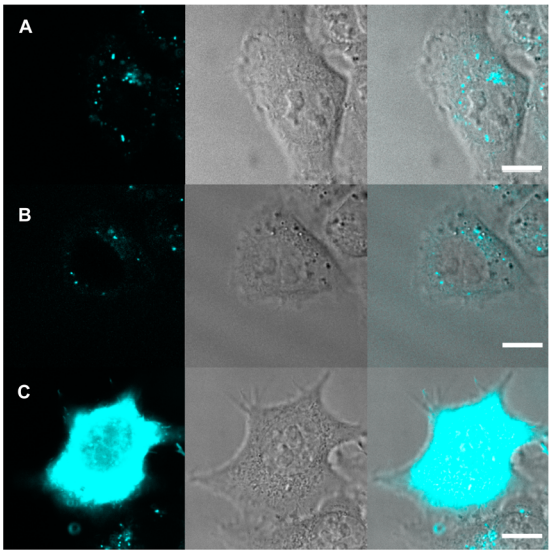

Figure 7. CLSM (left, 5% laser power), differential interference contrast (DIC, middle), and merged images (right) of HeLa cells after 15 min incubation with Cy5-CPP **1** (1 μM) without activators (A) and after preincubation for 5 min with 10 μM activator **7a** (B) and **7p** (C), all in Leibovitz medium at 37 °C. Scale bar: 10 μm.

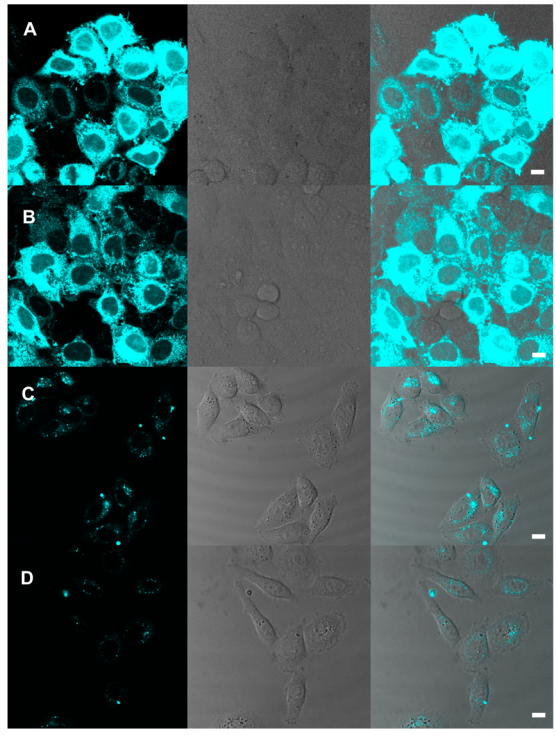

Figure 8. CLSM (left, 1% laser power for A, B, 5% for C, D), DIC (middle), and merged images (right) of HeLa cells after 5 min of incubation with activator **13** (A), **14** (B), **15** (C), and **16** (D, 10 μM each) and then 15 min with Cy5-CPP **1** (1 μM) in Leibovitz medium at 37 °C. Scale bar: 10 μm.

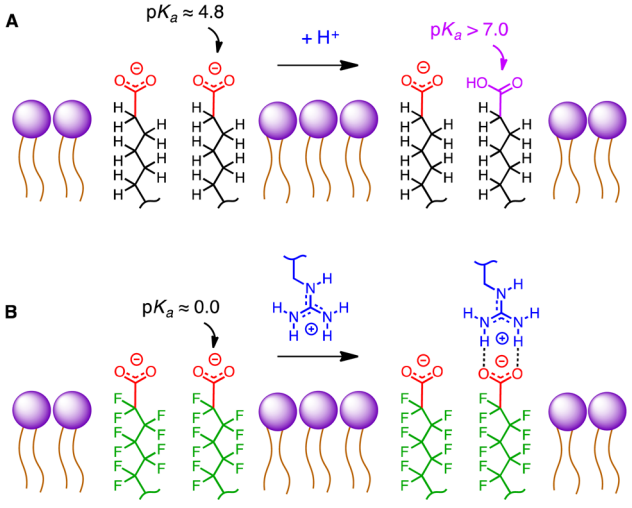

Figure 9. Fluorophilic CPP activators that operate with repulsion-driven ion-pairing interactions: (A) More basic carboxylates minimize charge repulsion between self-assembled activators by protonation. (B) Less basic carboxylates minimize charge repulsion between self-assembled activators by repulsion-driven ion pairing, i.e., the very stable yet sufficiently labile binding of CPPs (compare Figure 1).

CPPs, resulting in better uptake in cells, whereas antiparallel ionpair–π activators are much less active and give cellular distributions as for CPP **1** without activators (Figure 6). Control experiments with activators only confirmed that the observed fluorescence originates from the Cy5 attached to CPP **1** and not from the much weaker ANI fluorophore (Figure S4).

Similar trends were observed with activators **11** with perfluorinated tails. CPP uptake with parallel ionpair–π interactions in activator **11p** was clearly better than with antiparallel ionpair–π interactions in activators **11a** (Figure S5). Moreover, fluorous ionpair–π activators **11p** enabled CPP uptake in larger populations of cells in comparison to nonfluorinated activators **7p**. This increased apparent activity of ionpair–π activators **11** with fluorous tails could possibly originate from fluorophilic self-assembly[18] in cell membranes. To elaborate on this hypothesis, CPP activation by pure fluorophiles **13** and **14** was explored. Under the conditions developed for ionpair–π activators, uptake experiments with CPP **1** in the presence of perfluorinated fatty acids **13** and **14** gave highly fluorescent HeLa Kyoto cells (Figure 8A, B). Compared to results with ionpair–π activators, perfluorinated fatty acids **13** and **14** delivered CPP **1** more evenly to most cells. Fluorophile-activated CPPs appeared to localize preferentially in intracellular membranes. Significant diffuse overall fluorescence indicated CPP release into the cytosol, whereas the nuclei were much less fluorescent (Figures 8A, B).

Polyfluorinated fatty acids **15** and **16** did not activate CPP **1** for uptake into HeLa cells. The CLSM images showed weak fluorescence with a distribution similar to Cy5-CPP **1** in the absence of any activator (Figure 8C, D). This inactivity of controls **15** and **16** provided direct experimental support that activators **13** and **14** operate by repulsion-driven ion-pairing interactions with self-assembled fluorophiles (Figure 9). Namely, the fluorous self-assembly of activators in membranes will bring their negative charges into close proximity. The resulting proximity effects should be exactly complementary to those that account for the productive mode of action of CPPs (Figure 1C). Strongly basic bundles of anions will overcome charge repulsion by protonation (Figure 9A). "Unprotonatable," weakly basic bundles of anions will strongly bind counterions (Figure 9B). Examples for the protonation of proximal carboxylates at pH 7 include acid catalysis in glycosidases or proteases,[2] self-assembled fatty acids from premicellar aggregates to soap bubbles,[22] and so on. Repulsion-driven ion-pairing interactions with weakly basic, unprotonat-

DOI: 10.1021/jacs.6b06253
J. Am. Chem. Soc. 2016, 138, 11264–11271

able oligophosphodiesters (DNA, RNA, etc.) afford cation transporters and sensors in bulk and lipid bilayer membranes[2] and are the basis of all approaches to DNA/RNA delivery that operate with lipoplexes.[2]

In amphiphiles **15** and **16**, the absence of fluorines on the proximal carbons increases the basicity of the carboxylates. Fluorophilic self-assembly[18] in cell membranes thus fails to increase their activity because of proximity-induced protonation (Figure 9A). The recent observation that ordinary fatty acids can activate CPPs under basic conditions,[11] not under neutral, was consistent with this interpretation, suggesting that these fatty acids self-assemble in the membrane and minimize charge repulsion by protonation at pH = 7[22] and by CPP binding only at pH > 7.

Under physiological conditions, the fluorous fatty acids **13** and **14** offer the perfect combination of fluorophilicity and "unprotonatable" carboxylates. Complementary to guanidinium cations in CPPs (Figure 1C), these weaker bases generate operational repulsion-driven ion-pairing interactions in response to fluorophilic self-assembly[18] in cell membranes (Figure 9B). The result is most efficient CPP uptake (Figure 8). The cumulation of repulsion-driven ion-pairing interactions from self-assembled perfluorinated fatty acids on the one side and CPPs on the other side could also explain the apparent accumulation in intracellular membranes: Release into the cytosol by exchange with hydrophilic polyanions could become increasingly difficult (Figures 9B, 1F).

Interestingly, the most powerful activation of CPPs by repulsion-driven ion pairing with self-assembled perfluorinated fatty acids in HeLa cells was not predictable from transport experiments in vesicles. In these model systems, polyfluorinated fatty acids **13**–**16** were all similarly inactive, independent of the basicity of the carboxylate (Figure 5A). This was in clear contrast to ionpair–π activators including perfluorinated fatty acid **11**, which showed clear preference for parallel over antiparallel activators in vesicles and cells. This important difference was, however, understandable and meaningful considering the different processes detected in vesicles and cells. In CF-loaded vesicles, the export of intravesicular CF is monitored. Detailed studies, including positive controls in bulk membranes and anionic lipids as activators in bilayer membranes, provided experimental support that the export of anionic CF by pR–activator complexes occurs via counterion exchange.[2,4] In competition with ionpair–π activators, this ion exchange on the CPP scaffold is as unproblematic as with all other anionic activators tested previously. With the cumulation of repulsion-driven ion-pairing interactions in both self-assembled fluorophiles and CPPs, the temporary substitution of one or more of the tightly bound activators by CF becomes more difficult. As a result, CF export from CF-loaded vesicles does not occur. In clear contrast, occurrence and detection of cellular uptake does not require exchange of one or more activators in CPP–activator complexes with an anionic fluorophore. This mechanistic difference thus explains why with conventional activator–CPP complexes, uptake is predictable from vesicles, and with stronger activator–CPP complexes, cellular uptake is possible and detectable, whereas CF transport in vesicles is not.

The mode of action of fluorous CPP activators implied that differences in carboxylate basicity could possibly account also for the differences in activity between parallel and antiparallel ionpair–π activators. Anion–π interactions have been found to cause basicity changes up to $\Delta pK_a = 5.5$.[23] However, the weak π acidity of push–pull ANIs and the nearly identical spectroscopic properties of parallel and antiparallel ionpair–π activators in membranes (Figure 5C) did not support this conceivable alternative interpretation.

CONCLUSIONS

The concept of CPP activators has been introduced as early as 2003.[4] Reminiscent of catalysts, activators were expected to accelerate direct translocation of CPPs across lipid bilayer membranes and thus overcome endosomal capture. However, significant activation of CPPs to enter cells at pH 7 without endosomal capture has been limited so far to one example, i.e., pyrenebutyrate.[13] This report introduces more CPP activators that work in cells. Most importantly, their design is rational and conceptually innovative, aiming to apply lessons from supramolecular chemistry to cellular uptake.

Repulsion-driven ion-pairing interactions,[4] stable and labile at the same time, account for the counterion hopping that allows CPPs to move across the hydrophobic membrane barriers.[2,4] Perfluorinated fatty acids, the most powerful activators discovered in this study, offer repulsion-driven ion-pairing interactions also from the activator side. They combine the fluorophilicity[18] to self-assemble in the membrane with the poor basicity needed to attract CPPs with repulsion-driven ion-pairing interactions. The best fluorophilic activators, as simple as perfluorinated lauric acid, are shown to enable most efficient delivery of fluorescently labeled octaarginines into HeLa cells without endosomal capture. The excellent performance of fluorophilic activators in cells is not reproduced in model vesicles, presumably because assays in CF-loaded vesicles report on CPP-mediated anion export rather than CPP uptake. New assays reporting directly on CPP uptake in model membranes would be desirable.

Parallel ionpair–π interactions[12] are found to contribute to CPP activation, whereas antiparallel ionpair–π interactions inhibit CPP activators in model vesicles and in cell. Parallel ionpair–π activators cause exceptionally efficient CPP uptake into some cells, which become highly fluorescent, whereas other cells remain untouched. Although consistent with theoretical predictions and pertinent controls, including binding studies to membranes and CPPs, it could not be expected that the difference between parallel and antiparallel ionpair–π interactions would be so dramatic. Despite remarkably consistent results, it is thus important to reiterate that direct evidence for operational ionpair–π interactions for CPP activation is probably inaccessible. Contributions from other effects should never be fully excluded.

In summary, these results introduce repulsion-driven ion-pairing and parallel ionpair–π interactions as innovative concepts to elaborate on CPP activators. Naturally, these results also support counterion-mediated uptake with repulsion-driven ion-pairing interactions as the productive mode of action of arginine-rich CPPs.[2,4] Application of the lessons learned should enable rapid progress with the development of CPP activators for general use in practice.

ASSOCIATED CONTENT

Supporting Information

The Supporting Information is available free of charge on the ACS Publications website at DOI: 10.1021/jacs.6b06253.

Experimental details (PDF)

DOI: 10.1021/jacs.6b06253
J. Am. Chem. Soc. 2016, 138, 11264–11271

AUTHOR INFORMATION

Corresponding Author

*stefan.matile@unige.ch

Present Address

§Aichi Institute of Technology, Aichi 470-0392, Japan

Notes

The authors declare no competing financial interest.

ACKNOWLEDGMENTS

We thank the NMR, the Sciences Mass Spectrometry (SMS) and the imaging platforms for services, A. Roux and G. Gasparini for access to and assistance with cell culture and the University of Geneva, the European Research Council (ERC Advanced Investigator), the Swiss National Centre of Competence in Research (NCCR) Chemical Biology, the NCCR Molecular Systems Engineering and the Swiss NSF for financial support.

REFERENCES

(1) (a) Bartolami, E.; Bouillon, C.; Dumy, P.; Ulrich, S. *Chem. Commun.* **2016**, *52*, 4257−4273. (b) Priegue, J. M.; Crisan, D. N.; Martínez-Costas, J.; Granja, J. R.; Fernandez-Trillo, F.; Montenegro, J. *Angew. Chem., Int. Ed.* **2016**, *55*, 7492−7495. (c) McKinlay, C. J.; Waymouth, R. M.; Wender, P. A. *J. Am. Chem. Soc.* **2016**, *138*, 3510−3517. (d) Li, M.; Schlesiger, S.; Knauer, S. K.; Schmuck, C. *Angew. Chem., Int. Ed.* **2015**, *54*, 2941−2944. (e) DeRonde, B. M.; Birke, A.; Tew, G. N. *Chem. - Eur. J.* **2015**, *21*, 3013−3019. (f) Douat, C.; Aisenbrey, C.; Antunes, S.; Decossas, M.; Lambert, O.; Bechinger, B.; Kichler, A.; Guichard, G. *Angew. Chem., Int. Ed.* **2015**, *54*, 11133−11137. (g) Brock, R. *Bioconjugate Chem.* **2014**, *25*, 863−868. (h) Eggimann, G. A.; Blattes, E.; Buschor, S.; Biswas, R.; Kammer, S. M.; Darbre, T.; Reymond, J. L. *Chem. Commun.* **2014**, *50*, 7254−7257. (i) Bechara, C.; Sagan, S. *FEBS Lett.* **2013**, *587*, 1693−1702. (n) Inoue, M.; Tong, W.; Esko, J. D.; Tor, Y. *ACS Chem. Biol.* **2013**, *8*, 1383−1388. (j) Tang, H.; Yin, L.; Kim, K. H.; Cheng, J. *Chem. Sci.* **2013**, *4*, 3839−3844. (k) Nakase, I.; Akita, H.; Kogure, K.; Gräslund, A.; Langel, Ü.; Harashima, H.; Futaki, S. *Acc. Chem. Res.* **2012**, *45*, 1132−1139. (l) Ornelas-Megiatto, C.; Wich, P. R.; Fréchet, J. M. *J. Am. Chem. Soc.* **2012**, *134*, 1902−1905. (m) Appelbaum, J. S.; LaRochelle, J. R.; Smith, B. A.; Balkin, D. M.; Holub, J. M.; Schepartz, A. *Chem. Biol.* **2012**, *19*, 819−830. (n) Piest, M.; Engbersen, J. F. J. *J. Controlled Release* **2011**, *155*, 331−340. (o) Kolonko, E. M.; Pontrello, J. K.; Mangold, S. L.; Kiessling, L. L. *J. Am. Chem. Soc.* **2009**, *131*, 7327−7333. (p) McNaughton, B. R.; Cronican, J. J.; Thompson, D. B.; Liu, D. R. *Proc. Natl. Acad. Sci. U. S. A.* **2009**, *106*, 6111−6116. (q) Torchilin, V. P. *Adv. Drug Delivery Rev.* **2008**, *60*, 548−558. (r) Gump, J. M.; Dowdy, S. F. *Trends Mol. Med.* **2007**, *13*, 443−448. (s) Fernandez-Carneado, J.; Van Gool, M.; Martos, V.; Castel, S.; Prados, P.; De Mendoza, J.; Giralt, E. *J. Am. Chem. Soc.* **2005**, *127*, 869−874. (t) Fillon, Y.; Anderson, J.; Chmielewski, J. *J. Am. Chem. Soc.* **2005**, *127*, 11798−11803. (u) Zhou, P.; Wang, M.; Du, L.; Fisher, G. W.; Waggoner, A.; Ly, D. H. *J. Am. Chem. Soc.* **2003**, *125*, 6878−6879.

(2) Gasparini, G.; Bang, E.-K.; Montenegro, J.; Matile, S. *Chem. Commun.* **2015**, *51*, 10389−10402.

(3) Sakai, N.; Sordé, N.; Das, G.; Perrottet, P.; Gerard, D.; Matile, S. *Org. Biomol. Chem.* **2003**, *1*, 1226−1231.

(4) Sakai, N.; Matile, S. *J. Am. Chem. Soc.* **2003**, *125*, 14348−14356.

(5) Herce, H. D.; Garcia, A. E.; Litt, J.; Kane, R. S.; Martin, P.; Enrique, N.; Rebolledo, A.; Miles, V. *Biophys. J.* **2009**, *97*, 1917−1925.

(6) (a) Gasparini, G.; Bang, E.-K.; Molinard, G.; Tulumello, D. V.; Ward, S.; Kelley, S. O.; Roux, A.; Sakai, N.; Matile, S. *J. Am. Chem. Soc.* **2014**, *136*, 6069−6074. (b) Fu, J.; Yu, C.; Li, L.; Yao, S. Q. *J. Am. Chem. Soc.* **2015**, *137*, 12153−12160.

(7) Schmidt, D.; Jiang, Q. X.; MacKinnon, R. *Nature* **2006**, *444*, 775−779.

(8) Whitney, M.; Savariar, E. N.; Friedman, B.; Levin, R. A.; Crisp, J. L.; Glasgow, H. L.; Lefkowitz, R.; Adams, S. R.; Steinbach, P.; Nashi, N.; Nguyen, Q. T.; Tsien, R. Y. *Angew. Chem., Int. Ed.* **2013**, *52*, 325−330.

(9) Okuro, K.; Sasaki, S.; Aida, T. *J. Am. Chem. Soc.* **2016**, *138*, 5527−5530.

(10) Rothbard, J. B.; Jessop, T. C.; Lewis, R. S.; Murray, B. A.; Wender, P. A. *J. Am. Chem. Soc.* **2004**, *126*, 9506−9507.

(11) Herce, H. D.; Garcia, A. E.; Cardoso, M. C. *J. Am. Chem. Soc.* **2014**, *136*, 17459−17467.

(12) Fujisawa, K.; Humbert-Droz, M.; Letrun, R.; Vauthey, E.; Wesolowski, T. A.; Sakai, N.; Matile, S. *J. Am. Chem. Soc.* **2015**, *137*, 11047−11056.

(13) (a) Takeuchi, T.; Kosuge, M.; Tadokoro, A.; Sugiura, Y.; Nishi, M.; Kawata, M.; Sakai, N.; Matile, S.; Futaki, S. *ACS Chem. Biol.* **2006**, *1*, 299−303. (b) Candan, G.; Michiue, H.; Ishikawa, S.; Fujimura, A.; Hayashi, K.; Uneda, A.; Mori, A.; Ohmori, I.; Nishiki, T.; Matsui, H.; Tomizawa, K. *Biomaterials* **2012**, *33*, 6468−6475.

(14) Fujisawa, K.; Beuchat, C.; Humbert-Droz, M.; Wilson, A.; Wesolowski, T. A.; Mareda, J.; Sakai, N.; Matile, S. *Angew. Chem., Int. Ed.* **2014**, *53*, 11266−11269.

(15) (a) Dougherty, D. A. *Acc. Chem. Res.* **2013**, *46*, 885−893. (b) Mahadevi, A. S.; Sastry, G. N. *Chem. Rev.* **2013**, *113*, 2100−2138.

(16) (a) Giese, M.; Albrecht, M.; Rissanen, K. *Chem. Commun.* **2016**, *52*, 1778−1795. (b) Chifotides, H. T.; Dunbar, K. R. *Acc. Chem. Res.* **2013**, *46*, 894−906. (c) Ballester, P. *Acc. Chem. Res.* **2013**, *46*, 874−884. (d) Frontera, A.; Gamez, P.; Mascal, M.; Mooibroek, T. J.; Reedijk, J. *Angew. Chem., Int. Ed.* **2011**, *50*, 9564−9583. (e) Wang, D.-X.; Wang, M.-X. *Chimia* **2011**, *65*, 939−943.

(17) Zhao, Y.; Beuchat, C.; Mareda, J.; Domoto, Y.; Gajewy, J.; Wilson, A.; Sakai, N.; Matile, S. *J. Am. Chem. Soc.* **2014**, *136*, 2101−2111.

(18) (a) Marsh, E. N. G. *Acc. Chem. Res.* **2014**, *47*, 2878−2886. (b) Krafft, M. P.; Riess, J. G. *Chem. Rev.* **2009**, *109*, 1714−1792. (c) Zhang, W.; Curran, D. P. *Tetrahedron* **2006**, *62*, 11837−11865.

(19) See SI.

(20) Bhosale, S.; Matile, S. *Chirality* **2006**, *18*, 849−856.

(21) Sakai, N.; Takeuchi, T.; Futaki, S.; Matile, S. *ChemBioChem* **2005**, *6*, 114−122.

(22) Kanicky, J. R.; Shah, D. O. *Langmuir* **2003**, *19*, 2034−2038.

(23) Miros, F. N.; Zhao, Y.; Sargsyan, G.; Pupier, M.; Besnard, C.; Beuchat, C.; Mareda, J.; Sakai, N.; Matile, S. *Chem. - Eur. J.* **2016**, *22*, 2648−2657.

DOI: 10.1021/jacs.6b06253
J. Am. Chem. Soc. 2016, 138, 11264−11271